PROCEEDINGS OF SCIENCE

Measurement of the double polarization observables E and G at the Crystal Ball experiment at MAMI

Farah Noreen Afzal* **for the A2 collaboration**
Helmholtz-Institut für Strahlen- und Kernphysik, Universität Bonn
E-mail: afzal@hiskp.uni-bonn.de

The understanding of the nucleon excitation spectra requires the measurement of several polarization observables in addition to the unpolarized cross section. The Crystal Ball experiment at MAMI has measured for the first time the double polarization observables E and G simultaneously within one beam time. The simultaneous production of linearly (needed for G) and circularly (needed for E) polarized bremsstrahlung photons was achieved by using a longitudinally polarized electron beam together with a thin diamond foil as a radiator. Additionally, the Mainz frozen spin polarized target developed in cooperation with Dubna was utilized for the measurement. For the detection of the final state particles the Crystal Ball and the TAPS calorimeters were used. The obtained data was analyzed in respect to the π^0 final state and the preliminary results for the double polarization observables E and G are presented.

XVIth International Workshop in Polarized Sources, Targets, and Polarimetry, PSTP2015,
14-18 September 2015,
Bochum, Germany

*Speaker.

PoS(PSTP2015)036

1. Introduction

In order to understand Quantum Chromodynamics (QCD) in the non-perturbative regime, it is important to investigate the excitation spectra of nucleons. Until now, discrepancies exist between phenomenological quark model predictions [1, 2] or lattice QCD calculations [3] and experimentally observed states. In order to understand these discrepancies photoproduction reactions have been studied at several facilities like ELSA, GRAAL, Jefferson Lab and MAMI over the last years. Unpolarized cross sections have been measured and published for many photoproduction reactions with high precision. However, for an unambiguous determination of the partial wave amplitudes additional single and double polarization observables need to be measured as well [4] e.g. using a polarized photon beam and a polarized target (compare table 1 in [5]). Usually the double polarization observables E and G are measured in separate beam times using either circularly or linearly polarized photons [6, 7]. The A2 collaboration in Mainz attempted to simultaneously measure both observables for the first time.

2. Polarized beam and polarized target

For the presented data, the Mainz Microtron (MAMI) accelerator [8] delivered a longitudinally polarized electron beam of $E_0 = 1.557$ GeV energy. The electrons hit a thin diamond radiator foil producing either coherent or incoherent bremsstrahlung photons. The electrons were deflected in the magnetic field (1.8 T) of the Glasgow Photon Tagger [9] and hit the focal plane plastic scintillator detectors. The produced bremsstrahlung photons were collimated with a 2 mm collimator and impinged on the frozen-spin butanol target [10] located at the center of the Crystal Ball detector [11].

2.1 Linearly and circularly polarized photons

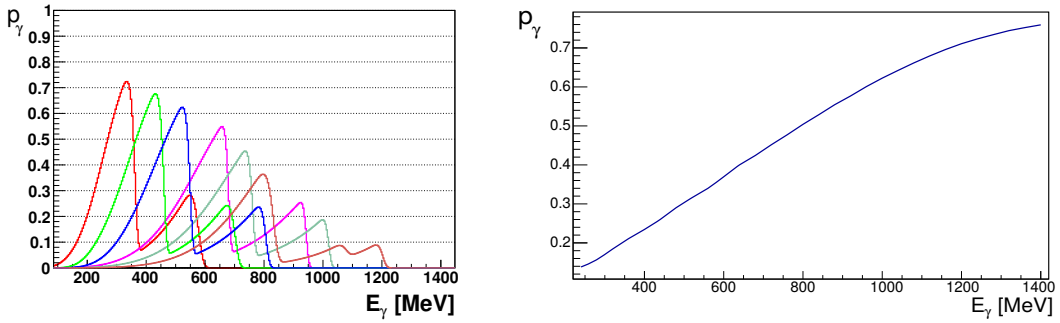

Figure 1: Left: The linear polarization degree for six different coherent peak settings: 350 MeV - 850 MeV. **Right:** The calculated circular polarization degree as a function of the photon beam energy. The calculation uses the measured electron polarization degree.

Linearly polarized photons are usually produced by coherent bremsstrahlung of unpolarized electrons using a crystal radiator like a diamond radiator. Circularly polarized photons can be produced as long as longitudinally polarized electrons are incident on any radiator. During data taking, longitudinally polarized electrons were used in combination with a diamond radiator which

produced an elliptically polarized photon beam with a linear and a circular polarization component. Thus allowing to measure the double polarization observables G and E at the same time.
Through alignment of the diamond with respect to the electron beam the coherent peak position was set at six different energies: 350 MeV - 850 MeV (see figure 1). A large energy range could be covered thereby. Data runs were taken with two perpendicular settings for the polarization plane in order to eliminate systematic effects. The linear polarization degree was determined according to [12].
The circular polarization degree highly depends on the polarization degree of the electron beam and the energy of the produced photons. The electron polarization degree was measured daily with a Mott measurement at the MAMI accelerator [13]. Figure 1 shows on the right the calculated circular polarization degree as a function of the photon beam energy as described in [14].

2.2 Frozen spin butanol target

For the target material butanol (C_4H_9OH) pellets [15] were chosen that were placed in a target cell of 2 cm length (see figure 2). The target cell is located inside of a ^{3}He/^{4}He dilution refrigerator that was developed in cooperation with the Joint Institute for Nuclear Research (JINR) Dubna [16]. For the target nucleon polarization process the Crystal Ball detector was moved away and replaced by a 2.5 T magnet which leads to a high electron polarization degree of the target material. Through irradiation of 70 GHz microwaves the electron polarization is transferred to the butanol protons via Dynamic Nucleon Polarization (DNP) [17]. During data taking, the Crystal Ball detector was moved back to its position surrounding the target (see figure 3) and an inner holding coil was used to provide a magnetic field of 0.68 T. This relatively low magnetic field together with the 25 mK temperature provided by the dilution refrigerator was sufficient to ensure long relaxation times of up to 2000 h before re-polarization of the target was required. For the initial polarization degree values of up to 90% are reachable. It is important to note that only the hydrogen nuclei of the butanol material can be polarized. In order to study background contributions from unpolarized carbon nuclei, data with a carbon foam target (see figure 2), which was inserted into the cryostat, were also taken.

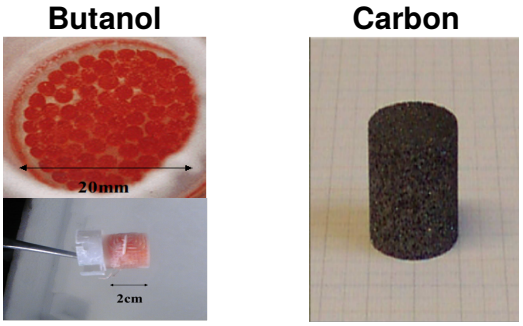

Figure 2: Left: Frozen butanol pellets inside the target cell. **Right:** Carbon foam target.

3. Particle detection and reconstruction

The final state particles were detected with two electromagnetic calorimeters: The Crystal Ball

detector [11] consisting of 672 NaI(Tl) crystals and the TAPS detector which is comprised of 366 BaF_2 and 72 $PbWO_4$ crystals [18]. Combined both detectors cover a polar angular range of 1° - 160° and allow time, energy and also polar and azimuthal angular measurement of the detected particles. Additionally, the comparison of the deposited energy in the 24 plastic scintillating strips of the Particle Identification Detector (PID) to the deposited energy in the Crystal Ball detector in a dE-E plot can help to distinguish between electrons/positrons, charged pions and protons. The same can be achieved in forward direction using the deposited energy in the plastic scintillating plates mounted in front of the TAPS elements (Vetos) to the TAPS energy deposition. The MWPCs are used to identify charged particles and to further increase the angular resolution of charged particles' tracks.

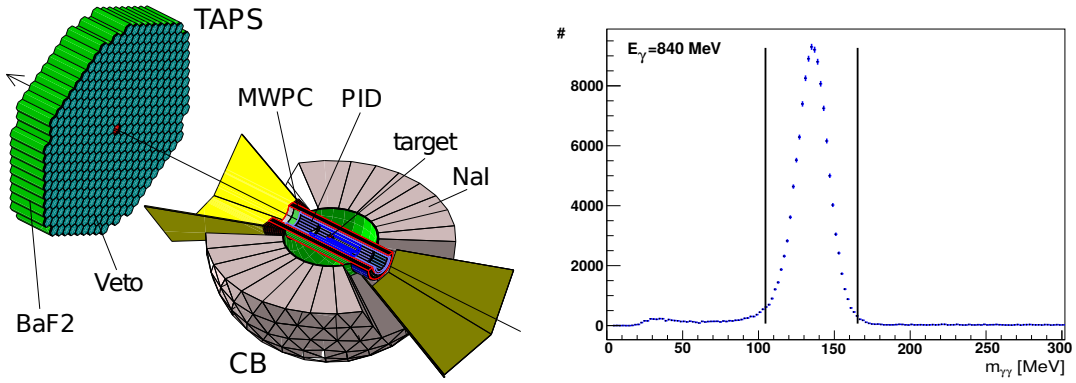

Figure 3: Left: The experimental setup consists of the Crystal Ball and the TAPS calorimeters. The PID, MWPC in the center of Crystal Ball and Vetos in front of the TAPS elements allow the identification of charged particles. **Right:** The invariant mass of two photons measured with the butanol target (blue points).

The $\gamma p \to p\pi^0 \to p\gamma\gamma$ candidates were selected by demanding time coincidence of all final state particles to the beam photon and additional energy dependent, 3σ kinematic cuts were used to reduce background. These kinematic cuts comprise cuts on the invariant mass of two photon candidates, the calculated proton mass using the known initial state and the four-momenta of the two final state photons, the azimuthal angle difference between the proton candidate and the π^0 candidate and the comparison of the polar angle of the measured and calculated charged particle. The invariant mass of the two photons is plotted in figure 3 on the right showing a clear π^0 peak after the application of all cuts for an energy of $E_\gamma = 840 \pm 20$ MeV and a low remaining background. The carbon data was scaled to the butanol data and subtracted for each energy bin. The selected events were used to extract the double polarization observables E and G using a similar approach as given in [6, 7].

4. Preliminary results for E and G

Preliminary results of the double polarization observable E in the photoproduction reaction $\gamma p \to p\pi^0$ were extracted from data runs utilizing a diamond radiator and are shown in figure 4 and 5. During the beam time data runs were also taken with an amorphous radiator instead of a diamond. An amorphous radiator can only produce circularly polarized photons and is usually employed to measure the double polarization observable E [7]. A comparison of results obtained

with a diamond radiator to results using an amorphous radiator shows an overall good agreement including the energy range of high linear polarization degree (see figure 4). Thus the preliminary results indicate that the circular polarization degree can be calculated for coherent bremsstrahlung in the same way as for incoherent bremsstrahlung in a first approximation.

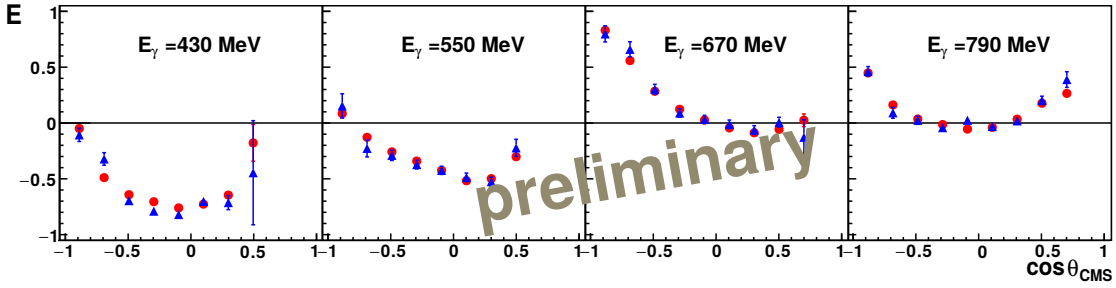

Figure 4: The double polarization observable E as a function of $\cos\theta_{CMS}$ for selected energy bins. The results obtained with a diamond radiator (red points) are compared to results obtained with an amorphous radiator (blue triangles).

In figure 5 the results for the double polarization observable E are further compared to data from the CBELSA/TAPS collaboration [7] and different partial wave analyses. The BnGa2014-02 partial wave analysis (PWA) solution [19] already used the E results of the CBELSA/TAPS collaboration [7] for the energy range of 600 MeV - 2300 MeV and is therefore not a prediction to the data in this energy range unlike the SAID-CM12 [20] and MAID [21] PWA solutions. The results are in good agreement with the existing data and mostly also with the different PWA solutions especially with the BnGa2014-02 PWA solution. Furthermore, the new data from the A2 collaboration is complementary to the existing data as it also covers the $\Delta(1232)$ resonance region.

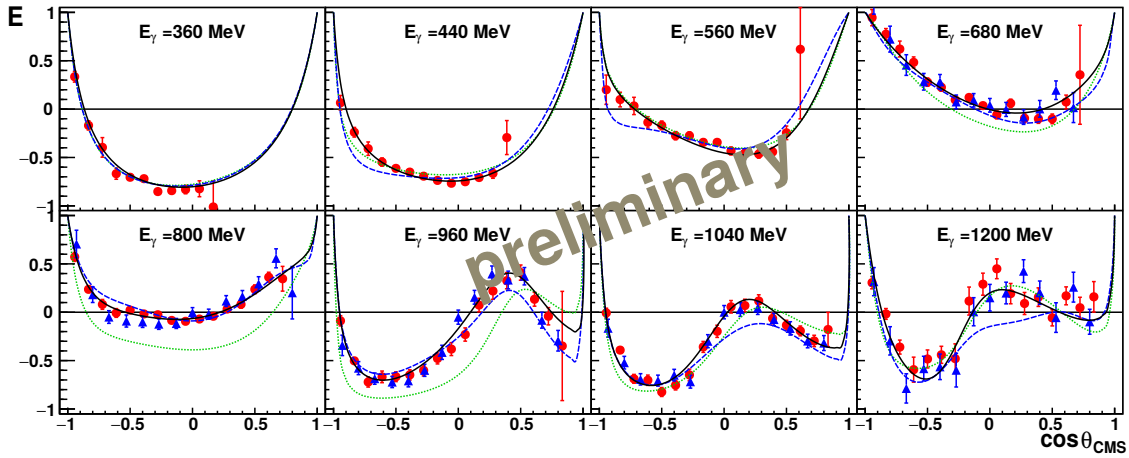

Figure 5: The double polarization observable E (red points) as a function of $\cos\theta_{CMS}$ for selected 40 MeV wide energy bins using a diamond radiator. The results are compared to CBELSA/TAPS data (blue triangles) [7], the BnGa2014-02 [19] (black solid line), SAID-CM12 [20] (dashed blue line) and MAID [21] (dotted green) partial wave solutions.

Figure 6 shows the double polarization observable G for selected energy bins. The results are again mostly compatible with the existing CBELSA/TAPS data [6] and the different PWA

solutions. It is noteworthy that only a small part (one sixth) of the data has been analyzed so far for the 650 MeV, 750 MeV and 850 MeV edge positions. The additional available data will significantly improve the statistics.

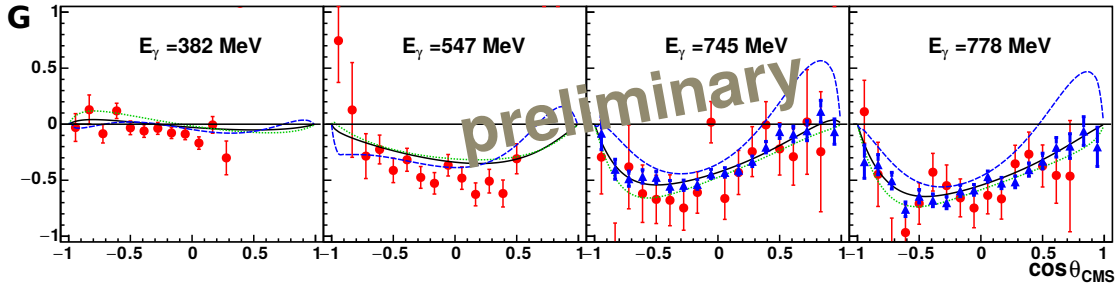

Figure 6: The double polarization observable G (red points) as a function of $\cos\theta_{CMS}$ for selected 33 MeV wide energy bins. The results are compared to CBELSA/TAPS data (blue triangles) [6], the BnGa2014-02 [19] (black solid line), SAID-CM12 [20] (dashed blue line) and MAID [21] (dotted green) partial wave solutions.

5. Conclusion

The double polarization observables E and G have been simultaneously measured at the Crystal Ball experiment at MAMI using a longitudinally polarized electron beam incident on a diamond radiator and a longitudinally polarized frozen spin target. The preliminary results are in agreement with existing data and additionally present first E and G data in the $\Delta(1232)$ resonance region.

6. Acknowledgement

We thank the staff of MAMI and all the participating institutions for their invaluable contributions to the success of the experiment. This work was supported by the Deutsche Forschungsgemeinschaft (SFB1044 and SFB/TR16), Schweizerischer Nationalfonds and HadronPhysics3 under the 7th Framework Program of the EU.

References

[1] S. Capstick and W. Roberts, , *Prog. Part. Nucl. Phys.* **45**, 241 (2000).

[2] U. Löhring, B. Ch. Metsch and H. R. Petry, *Eur. Phys. J. A* **10**, 395 (2001).

[3] R. G. Edwards, J. J. Dudek, D. G. Richards, and S. J. Wallace, *Phys. Rev. D* **84**, 074508A (2011).

[4] A. S. Omelaenko, *Sov. J. Nucl. Phys.* **34**, 406 (1981).
Y. Wunderlich et al., *Phys. Rev. C.* **89**, 055203 (2014).

[5] A. Thiel et al., in proceedings of *PSTP2015*, PoS(PSTP2015)046 (2016).

[6] A. Thiel et al., *Phys. Rev. Lett.* **109**, 102001 (2012).
A.Thiel et al., *EPJA*, to be published soon.

[7] M. Gottschall et al., *Phys. Rev. Lett.* **112**, 012003 (2014).
M. Gottschall et al., *EPJA*, to be published soon.

[8] K.-H. Kaiser et al., *Nucl. Instrum. Methods Phys. Res.* **A593**, 159 (2008).

[9] J. C. McGeorge et al., *Eur.Phys.J.* **A37**, 129 (2008).

[10] A. Thomas, *Eur. Phys. J. Spec. Top.* **198**, 171 (2011).

[11] A. Starostin et al., *Phys. Rev. C* **64**, 055205 (2001).

[12] K. Livingston, *Polarization from Coherent Bremsstrahlung Enhancement*, *CLAS NOTE 2011-020*.

[13] V. Tioukine, K. Aulenbacher, and E. Riehn, *Rev. Sci. Instrum.* **82**, 033303 (2011).

[14] A. H. Olsen and L. C. Maximon, *Phys. Rev.* **114**, 887 (1959).

[15] S. Goertz et al., in proceedings of *PSTP2015*, PoS(PSTP2015)009 (2016).

[16] Yu.A. Usov, *Frozen spin targets developed at Dubna. History and traditions*, in proceedings of *PSTP2015*, PoS(PSTP2015)021 (2016).

[17] D. G. Crabb and W. Meyer, *Annu. Rev. Nucl. Part. Sci.* **47**, 67 (1997).

[18] R. Novotny, *IEEE Trans. Nucl. Sci.* **38**, 379 (1991).

[19] E. Gutz et al., *Eur. Phys. J. A* **50**, 74 (2014).

[20] R.L. Workman, M.W. Paris, W.J. Briscoe, I.I. Strakovsky, *Phys. Rev. C* **86** 015202 (2012).

[21] D. Drechsel, S.S. Kamalov and L. Tiator, *Eur. Phys. J. A* **34**, 69 (2007) [arXiv:0710.0306[nucl-th]].